

Simulation of Boiler Drum Wall Temperature Differential and its Estimation¹

Prof Dr. Waladin K. Said²

Bashra Kadhim Oleiwi²

Abstract

This paper is concerned with the problem of boiler drum wall temperature estimation to limit thermal stresses. The boiler drum of AL-Mussiab thermal power station is taken as a case study. It deals with the fundamental issue that must be considered when applying a linear theory (i.e the Kalman filter) to practical non-linear problems. The Kalman filter is applied to estimate boiler drum wall temperature using the outer surface temperature of boiler drum wall (measurable) variable. The classical estimator (Kalman filter) is simple but it requires a good dynamic model to give reliable results. The numerical test results showed that the estimator is efficient and works well and it converges to the correct conditions (to within $\pm 1^\circ\text{C}$) in time about half an hour from boiler heating start up. The estimator is robust where 100% error in initial conditions did not seriously influence the transient time to produce correct estimated output.

Key words: Boiler drum wall modeling; Power station; Kalman filter application.

تمثيل و تخمين فرق درجات الحرارة لجدار وعاء المرجل البخاري

الخلاصة

يتناول البحث تخمين درجة الحرارة لجدار وعاء المرجل البخاري بإجراء قياسات غير مباشرة بهدف الحد من إجهاداته الحرارية عند التشغيل وقد استخدم وعاء مرجل محطة كهرباء المسيب الحرارية لأغراض هذه الدراسة. يتعامل البحث مع المفاهيم الأساسية التي يجب ان تؤخذ بنظر الاعتبار عند تطبيق النظرية الخطية (مثال: مرشح كالمان) للمشاكل العملية غير الخطية. أستخدم مرشح كالمان لتقدير درجة حرارة جدار وعاء مرجل محطة المسيب الحرارية بالأعتماد على مقياس واحد لدرجة حرارة السطح الخارجي لجدار الوعاء. المخمن الكلاسيكي (مرشح كالمان) بسيط لكنه يتطلب نموذج ديناميكي جيد لكي يعطي نتائج معتمدة. تشير نتائج الاختبار بأن المخمن المصمم كفو و جيد حيث بإمكانه تخمين درجة حرارة جدار وعاء المرجل خلال نصف ساعة من بدء عملية التشغيل و تشير الأختبارات النظرية بإمكانياته العالية حيث أن بالرغم من وجود 100% خطأ في الشروط الابتدائية للمخمن لم يتأثر ناتج التخمين بجديده على أداء المخمن للتوصل الى التخمين الصحيح لدرجات الحرارة.

1. This paper was presented in the Engineering Conference of Control, Computers and Mechatronics Jan. 30-31/2011, University of Technology.
2. Control & Systems Eng. Dept./ University of Technology, Baghdad, Iraq.

1- Introduction

The boiler is a major part in thermal power stations and since the boiler is the slowest responding part in the plant especially at starting up, the plant response is highly influenced by the boiler response. The procedure of starting up and shutting down the power station is limited by following the procedure of starting and shutting the boiler to prevent high thermal stresses [1,2].

Stresses in boiler equipment particularly those of the drum during transients limit the of thermal power plants. Short starting up time is desired to meet energy demand requirements. Furthermore boiler drum working environment is harsh, thus the probability of failure in the measurement system is high. Therefore, it is necessary to develop a state space model and optimal estimation of states, which would gradually improve the current state estimates by making use of the available on-line measurements for the drum wall temperature. This approach can make use of the Kalman filter procedure for observable systems, as it is for this case.

Kalman filter represents the most widely applied and demonstrably useful results to emerge from the state variable approach of "modern control theory"[3]. The Kalman filter has been the subject of extensive research and application, hence, orbit determination, tracking and navigation problems, represent probably, the first major applications of the Kalman filter. Estimation and control problems in industrial processes and power systems utilized Kalman filter extensively. It has been applied to the estimation of temperature and prediction of the ingot temperature in the soaking pit operations based on other available measurements Lumelsky [4]. A bank of Kalman filters (one for each instrument) in the design of an instrument failure detection system for a pressurized water reactor (PWR)

pressurizer was applied by Tylee [5]. A Kalman filter with extended models to estimate state variables (unmeasured temperatures in the glass melting furnace) was used by Huisman, *et. al.* [6]. A regular Kalman filter for continuous monitoring of induction furnace charge temperature based on a single furnace lining temperature measurement was developed by Sa'id and AL-Kubaissy [7]. Fluerasu and Sutton [8] designed and implemented a computer-controlled temperature tracking system which combines standard Proportional-Integral-Derivative (PID), thermal modeling and Kalman filtering of the temperature reading in order to reduce the noise.

This paper is concerned with the development of a practically feasible dynamic estimator (Kalman filter) which can be used to limit thermal stresses during power station boiler start up. In the following sections a mathematical model for the boiler drum temperature is derived for the starting up mode and the Kalman filter estimator is developed and evaluated numerically.

2-. System Description

The drum of the boiler is a thick wall cylinder used for separating the steam from steam-water mixture, as shown in figure (1). It is located at the top of the boiler and it is hanged by four hinges, two at each side and it is manufactured from steel alloy (SA 299). The steam-water mixture coming from riser tubes enter the drum via a number of cyclonics, which are used for increasing the rate of separation process as shown in figure (1). The separated steam is conveyed from the drum to the super heater through a set of pipelines. The intake points of these pipelines are uniformly distributed along the longitudinal direction at the top of the drum [2].

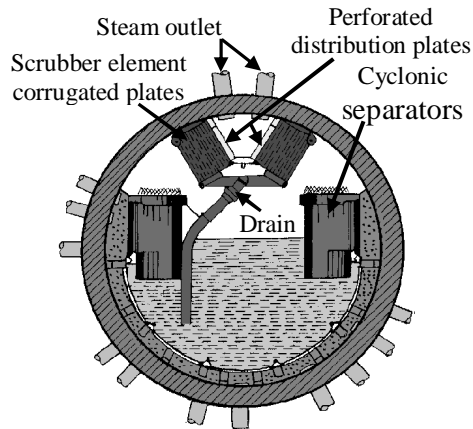


Figure (1) Cross section of Al-Mussiab boiler drum.

The boiler drum is subjected to thermal stresses due to the temperature difference between the inner and outer surfaces of the drum wall during starting up. Hence, the working speed of thermal power stations is limited by the maximum amount of permissible thermal stresses. There are “24” thermocouples located at different points on the drum wall used to monitor the stresses. The drum dimensions used in this work are detailed in Table (1).

Table (1): Drum dimensions used in this work [2].

Item	Dimension
Length	15 m
Inner Radius	0.9144 m
Outer Radius	1.0964 m
Thickness	0.182 m
Volume	42.3 m ³
Weight	172 ton

The structure of the proposed thermal stress control system to be developed is shown in figure (2). The control loop includes the estimator which produces the estimated values of the states and outputs for the next moment based on the measured values of the outputs at the current moment and the control effort at the previous moment.

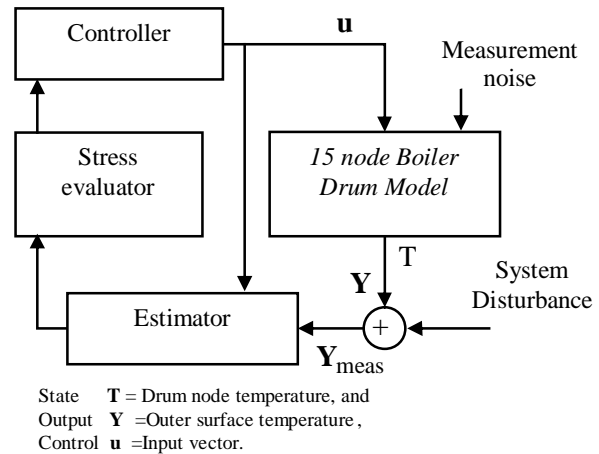


Figure (2) Boiler drum control system structure.

3- Boiler Drum Simulation Requirements

The coming sections are devoted to the simulation and the realization of the system shown in figure (2). The simulation is based on Matlab software.

A. Boiler Drum Wall Temperature Rise Modeling

For practical monitoring applications, the thermal system can be approximately represented by a lumped parameter system that can be described by ordinary differential equations. Such a set of linearised ordinary differential equations are much easier and faster to solve numerically. The lumped thermal model assumes that heat storage in a material can be represented by an effective thermal capacitance, C , and that the resistance to heat flow between two points can be represented by an effective thermal resistance, R , [9].

The lumped model approach results in first order dynamics in the temperature response to heat input at a given point or “node “. For a single node, the heat balance equation is simply given by [9];

$$q_i(t) = \frac{T(t) - T_a(t)}{R} + C \cdot \frac{dT(t)}{dt} \quad (1)$$

where T_a is the adjacent node temperature. Equation (1) may be put in state variable form, anticipating the construction of a set of dynamic equations describing temperature distribution in the drum wall, i.e.;

$$\dot{T} = \frac{1}{RC}(T_a(t) - T(t)) + \frac{q_i(t)}{C} \quad (2)$$

To obtain a set of linearized differential equations for the lumped parameter model, the single node described by equation (2) will be used.

The transient temperature variation in the shell material of the boiler drum is a two-dimensional case and the boundary conditions are dictated by the drum water level and temperature. The latter is, of course, dependent on the steam pressure. This assumes that there is no temperature gradient along the 15 m long boiler drum. Figure (3) shows one way in which the basic thermal network may be set on the drum wall.

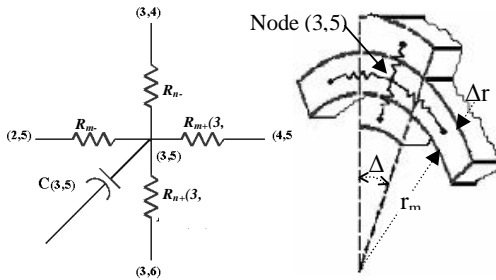


Figure (3) Equivalent R-C simulation for the boiler drum shell.

B. Boiler Drum Wall Thermal Dynamic Equations

For a two dimensional heat flow, and using the node (m,n) shown in figure (3), equation (2) takes the following form [10,11,12];

$$\dot{T}_{m,n} = (\psi_{m,n} + q_{m,n}) / C_{m,n} \quad (3)$$

Where m and n designate radial and circumferential number of nodes, and;

$$\psi_{m,n} = \sum_{i=+1 \& -1} ((T_{m+i,n} - T_{m,n}) / R_{m+i,n} + \beta_{m,n}),$$

where;

$$\beta_{m,n} = (T_{m,n+i} - T_{m,n}) / R_{m,n+i} .$$

$R_{m\pm i,n}$ = Radial thermal resistance.

$R_{m,n\pm i}$ = Circumferential thermal resistance.

$C_{m,n}$ = Node thermal capacitance

Writing equation (3) for each of the specified nodes leads to a system of first order dynamic equations. A computer program using MATLAB software was written to solve the set of first order differential equation using fourth order Runge Kutta method.

C. State Space and Measurement Equations of Boiler Drum

The system representations given by equation (3) are based on input and output variables and it is a linear model. It is convenient to obtain a simplified boiler drum model using state variables.

To derive the state space model, the number of states must be first determined. Equation (3) clearly shows that the states are the temperature of the nodes of the drum wall. The number of nodes depends on whether the problem is a one dimensional heat flow (radial heat flow) or a two dimensional heat flow (radial and circumferential heat flow). Increasing the number of nodes will improve the accuracy of the mathematical model of the boiler drum. We shall first divide the drum_wall radially into three nodes and assume radial heat flow only. Equation (3) will take the following equivalent state space model (general form);

$$\dot{T}(t) = A T(t) + B u(t) \quad (4)$$

where T is the drum wall temperature node state vector and u is the input vector. Using the drum dimension of AL-Mussiab boiler drum as given in Table (1) and the definition of R and C for 3 radial nodes and 20 circumferential nodes, equation (4) becomes;

$$\begin{bmatrix} \dot{T}_1 \\ \dot{T}_2 \\ \dot{T}_3 \\ \dots\dots\dots \\ \dot{T}_d \\ \dot{T}_{air} \end{bmatrix} = 10^{-3} \begin{bmatrix} -1594 & 075 & 0 \\ 07 & -1445 & 0745 \\ 0 & 07 & -0744 \\ \dots\dots\dots & \dots\dots\dots & \dots\dots\dots \\ 0844 & 0 \\ 0 & 0 \\ 0 & 0044 \end{bmatrix} \begin{bmatrix} T_1 \\ T_2 \\ T_3 \\ \dots\dots\dots \\ T_d \\ T_{air} \end{bmatrix} + \dots\dots\dots \quad (5)$$

Where T_d and T_{air} represent temperature of fluid inside drum and temperature of air outside drum (state input), respectively.

The discrete form of equation (4) is;

$$\mathbf{T}_k = \Phi_{k-1} \mathbf{T}_{k-1} + \mathbf{B}_{k-1} \mathbf{u}_{k-1} \quad (6)$$

$$\mathbf{Y}_k = \mathbf{H} \mathbf{T}_k \quad (7)$$

where;

$\mathbf{T}_{k-1}, \mathbf{T}_k$ =Plant state vectors at moments $k-1$ and k , respectively.

\mathbf{u}_{k-1} = Control variable vector at the moment $k-1$.

\mathbf{Y}_k = Output vector at moment k ,

k = Time index.

(Note: Along this paper $\mathbf{T}(k)= \mathbf{T}_k, \mathbf{Y}(k)= \mathbf{Y}_k, \mathbf{u}(k)= \mathbf{u}_k$).

For a sampling time of 1 second, the elements of equation (6) are;

$$\Phi_k = \begin{bmatrix} 0.9984 & 0.0007 & 0 \\ 0.0007 & 0.9986 & 0.0007 \\ 0 & 0.0007 & 0.9993 \end{bmatrix}, \quad \text{and}$$

$$\mathbf{B}_k = 10^{-3} \begin{bmatrix} 0.8429 & 0 \\ 0.0003 & 0 \\ 0 & 0.0438 \end{bmatrix}$$

To select the number of nodes for the drum wall in radial and circumferential directions, a set of numerical tests were made to examine the dynamic wall temperature response with various number of nodes in both directions (radial and circumferential).

The above study was concluded to adopt a mathematical model with 5 rings in radial direction and 20 sections in circumferential direction. Figure (4) shows the temperature time response of boiler drum wall. It illustrates the dynamic behavior of 5 nodes along the thickness of the drum wall at the starting up of the boiler with inner surface

temperature gradient of “0.54 °C/min”. This model was used as the mathematical model for Kalman filter design.

A fifteen nodes state apace model was also derived and used as a reference model for estimator’s performance. A set of models describing the dynamic behavior of the drum wall temperature for two dimensional heat flow case (radial and circumferential heat flow) were derived and are given in reference [12].

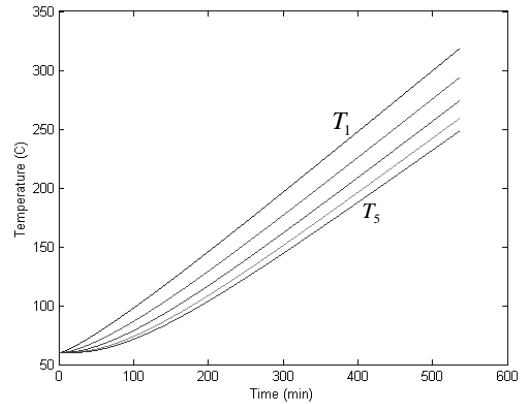


Figure (4) Temperature distribution of the 5 nodes of the drum wall with inner surface temperature gradient of “0.54°C/min” at starting up mode.

4- Kalman Filter

The Kalman filter is essentially a set of mathematical equations that implement a predictor-corrector type estimator. It is optimal in the sense that it minimizes the estimated error covariance [13]. Hence, it is the best linear estimator, which can produce an optimal estimate of the state of a linear dynamic system, subject to the disturbances having Gaussian distribution. The function of a filter is to separate the signal or information from the noise- corrupted data and it can be used to compute the optimal estimate of the signal [14].

The filter is initialized with an initial estimate of the signal and its error covariance. Then as each measurement becomes available in real time, it is used to update or refine the filter’s previous

estimate. Thus, the initial estimate is successively improved until, eventually; a steady state condition is reached where no further improvements are obtained [15].

In the implementation of a Kalman filter, a mathematical model of the signals to be estimated is described by means of linear stochastic difference equations. Equation (6) will assume the following form:

$$\mathbf{T}_k = \boldsymbol{\Phi}_{k-1} \mathbf{T}_{k-1} + \mathbf{B}_{k-1} \mathbf{u}_{k-1} + \mathbf{w}_{k-1} \quad (8)$$

The observation (measurement) of the process is assumed to occur at discrete points in time in accordance with the relationship.

$$\mathbf{Y}_k = \mathbf{H} \mathbf{T}_k + \mathbf{v}_k \quad (9)$$

Where \mathbf{w}_k and \mathbf{v}_k represent the process noise and measurement noise, respectively. They are assumed to be uncorrelated zero-mean, white noise sequences with known statistics whose properties are described by:

$$E[\mathbf{w}_k] = E[\mathbf{v}_k] = 0 \quad (10)$$

And joint covariance matrix;

$$E\left[\begin{pmatrix} \mathbf{w}_k \\ \mathbf{v}_k \end{pmatrix} \begin{pmatrix} \mathbf{w}_k^T & \mathbf{v}_k^T \end{pmatrix}\right] = E\left[\begin{bmatrix} \mathbf{Q}_k & 0 \\ 0 & \mathbf{R}_k \end{bmatrix}\right] \quad (11)$$

Where; \mathbf{Q} and \mathbf{R} are the process and measurement noise covariances and they are assumed constant [15].

The equations for the Kalman filter fall into two groups: time update equations and measurement update equations. The time update equations are responsible for projecting forward (in time) the current state and error covariance estimates to obtain the a priori estimates for the next time step. The measurement update equations are responsible for the feedback, i.e., for incorporating a new measurement into a priori estimate to obtain an improved a posteriori estimate. The time update equations can also be thought of as predictor equations, while the measurement update equations can be thought of as corrector equations. Indeed the final estimation algorithm resembles

that of a predictor-corrector algorithm for solving numerical problems. The time and measurement update equations are given below [13];

i-) *Discrete Kalman filter time update equations*

$$\hat{\mathbf{T}}_k^- = \boldsymbol{\Phi} \hat{\mathbf{T}}_{k-1} + \mathbf{B} \mathbf{u}_{k-1} \quad (12)$$

$$\mathbf{P}_k^- = \boldsymbol{\Phi} \mathbf{P}_{k-1} \boldsymbol{\Phi}^T + \mathbf{Q} \quad (13)$$

ii-) *Discrete Kalman filter measurement update equations*

$$\mathbf{K}_k = \mathbf{P}_k^- \mathbf{H}^T (\mathbf{H} \mathbf{P}_k^- \mathbf{H}^T + \mathbf{R})^{-1} \quad (14)$$

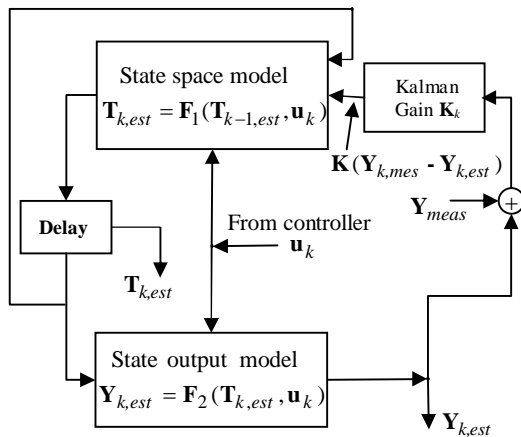
$$\hat{\mathbf{T}}_k = \hat{\mathbf{T}}_k^- + \mathbf{K}_k (\mathbf{Y}_k - \mathbf{H} \hat{\mathbf{T}}_k^-) \quad (15)$$

$$\mathbf{P}_k = (\mathbf{I} - \mathbf{K}_k \mathbf{H}) \mathbf{P}_k^- \quad (16)$$

Having an initial estimate $\hat{\mathbf{T}}_0$ and the initial estimation error (noise) covariance \mathbf{P}_0 and a model for the system and measurement, the recursive Kalman filter equations can be solved next (equations (12) to (16)). As can be seen from time update equations (12) and (13) the state and covariance estimates are projected forward from time step $k-1$ to k . However, the first task during the measurement update is to compute the Kalman gain, \mathbf{K}_k using equation (14). The next step is to actually measure the process to obtain \mathbf{Y}_k , and then to generate a posteriori state estimate by incorporating the measurement (equation (15)). The final step is to obtain a posteriori error covariance estimate via equation (16).

After each time and measurement update pair, the process is repeated with the previous a posteriori estimates used to project or predict the new a priori estimates. This recursive nature is one of the very appealing features of the Kalman filter, it makes practical implementations much more feasible than (for example) the Wiener filter. The Kalman filter recursively conditions the current estimate on all of the past measurements. A MATLAB program is designed to solve the problem and figure (5) gives a

pictorial overall structure of the computation scheme.



State \mathbf{T} = Drum wall l node temperature,
 Output \mathbf{Y} = Outer surface temperature,
 \mathbf{u} = Input vector .

Estimation equations

$$\mathbf{T}_{k,est} = \mathbf{A}\mathbf{T}_{k-1,est} + \mathbf{B}\mathbf{u}_k + \mathbf{K}(\mathbf{Y}_{k,meas} - \mathbf{Y}_{k,est})$$

$$\mathbf{Y}_{k,est} = \mathbf{H}\mathbf{T}_{k,est}$$

Figure (5) The overall structure of the estimator computation scheme.

5- Simulation

The Kalman filter scheme shown in figure (5) estimates the temperature difference between inner and outer surface during boiler starting up. F_1 and F_2 are given by equations (8) and (9), respectively.

The current work is concerned with the estimation of temperature difference between inner and outer surfaces using the 5 node model. The temperature measurement is taken from the 15 node model which is taken as the reference. Figure (6) clearly defines the symbols used where nodes (2) and (14) of the 15 node model correspond to nodes (1) and (5) of the 5 node model. That is temperatures T_2 and T_{14} of the 15 node model correspond to temperatures T_1 and T_5 of the 5 node model, respectively. For simplicity, the symbols *T_1 and *T_5 will be used instead of T_2 and T_{14} for the 15

node model. Also, the drum wall temperature difference Δ^*T_w , the reference, represents (${}^*T_1 - {}^*T_5$) whilst the estimated wall temperature difference is ΔT_w or ($T_1 - T_5$). Finally, Gaussian noise is added to the drum wall temperature measurement “ *T_1 and/or *T_5 ” to simulate measurement noise.

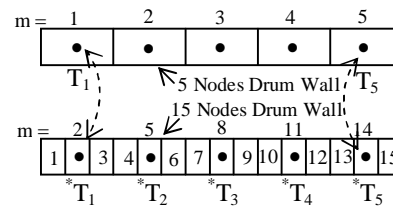


Figure (6) A comparative correspondence between 5 and 15 nodes models.

6- Boiler Drum Performance With Kalman Filter

A series of numerical experimental tests were carried out and figures (7) to (15) summarize the results. Figure (7a) shows the temperature difference behavior of the estimator using the 5 nodes model and the data obtained from the 15 nodes dynamic model. As was discussed above, the temperatures of the latter model are considered as real system temperatures. Hence, the field temperature measurement is taken using the outer node, i.e., *T_5 . Gaussian noise is added to *T_5 to simulate real temperature measurements. Based on this temperature measurement, the estimator estimates the wall temperature difference where the estimator initial conditions are $[60 \ 60 \ 60 \ 60 \ 60]^T$ °C. The figure shows very good tracking after about half an hour from boiler heating start up. The temperature difference between that estimated by the Kalman filter (ΔT_w) and the reference model (Δ^*T_w) is shown in figure (7b), where the peak error deviation is +3 and -5.2°C. From the results shown in figure (7b), the estimator performance is close to reference performance.

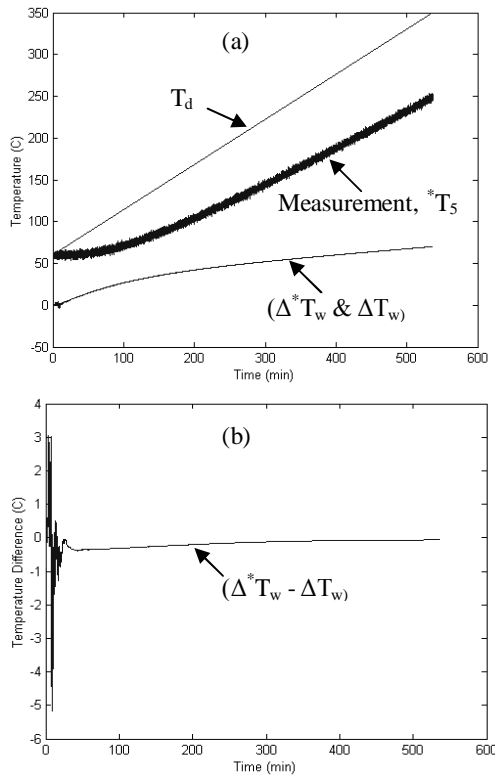


Figure (7) a) Estimator performance with T_5 node measurement. b) Estimated (Δ^*T_w) and drum wall differential (ΔT_w) difference.

Figure (8a) shows the performance of the estimator using measurements of the inner drum wall temperature (T_1 plus Gaussian noise). The difference between the reference temperature, Δ^*T_w , and estimated temperature, ΔT_w , is illustrated in figure (8b). The peak deviation (error) is +12.5 and - 4°C. Figure (8b) also shows that the performance of the estimator to follow the desired wall temperature differential is very good. A comparison between figures (7b) and (8b) reveals that the performance of the Kalman filter using outer drum wall temperature measurement (T_5) is superior to that when inner drum wall temperature measurement (T_1) is used. The former filter shows 50% reduction in maximum temperature deviation. A better estimator

performance is expected if both temperatures T_1 and T_5 are used.

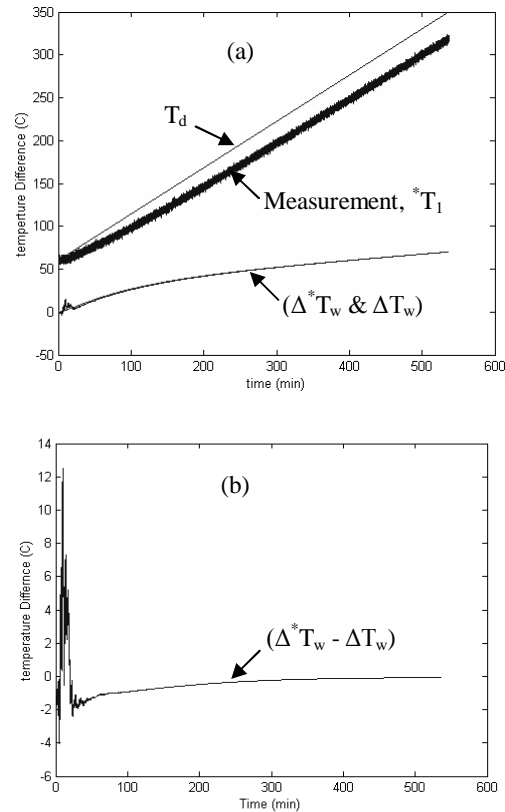


Figure (8) a) Estimator performance with T_1 node measurement. b) Estimated (Δ^*T_w) and drum wall differential (ΔT_w) difference.

The performance of the estimator using inner and outer wall temperature measurements is shown in figure (9a). The difference between the estimator and actual model wall temperature differentials $(\Delta^*T_w - \Delta T_w)$ is shown in figure (9b). It can be clearly seen that the maximum error is 0.42 °C which shows a marked improvement in performance. A comparison between the three cases above shows that the tracking is now faster due to the availability of more information by the measurement of T_1 and T_5 .

The performance of the three types of estimators can best be evaluated

by using the performance index (J_i), which is defined as [7];

$$J_i = \frac{1}{n} \sum_{i=1}^n |T_{est}(i) - T_{real}(i)| \quad (17)$$

where, $T_{est}(i)$ is the estimated temperature value at the i^{th} time point. $T_{real}(i)$ is the actual value of the temperature and n is the number of time points. The performance of the estimator is the average absolute deviation of the estimated temperature from the actual temperature. For initial estimator conditions of $[60 \ 60 \ 60 \ 60 \ 60]^T$, the estimator performance is rather poor at the beginning of the heating process and the quality of the estimation improves at the end of the heating process, as shown in figures (7), (8) and (9).

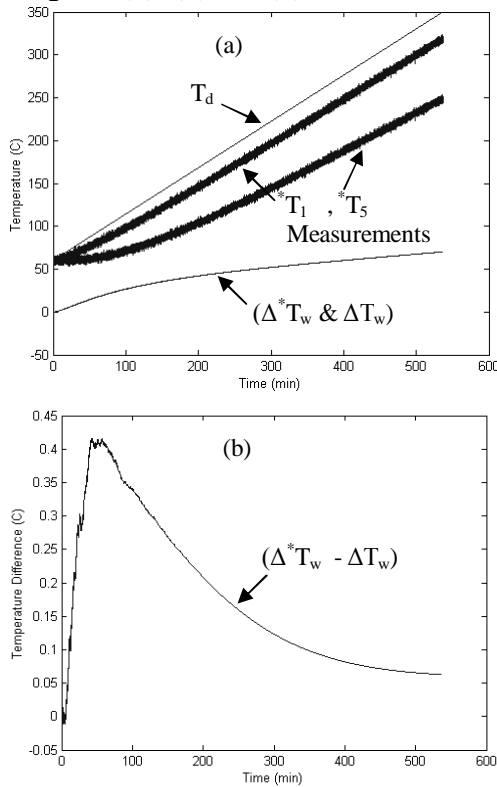


Figure (9) a) Estimator performance with T_1^* and T_5^* measurements. b) Estimated (ΔT_w^*) and drum wall differential (ΔT_w) difference.

The behavior of the estimator is investigated by evaluating the index (J_i)

for three time intervals. The test results are summarized in Table (2). The first interval is defined by the period “0-50 min” from start up. The second interval is defined by the remaining run time. Finally, the third interval covers overall run time. For the first interval, Table (2) clearly shows that the estimator with T_1^* and T_5^* measurements ($J_i=0.24$) is better than the other two estimators. Also, the estimator with T_5^* measurement ($J_i= 0.59$) is better than that with T_1^* measurement ($J_i=1.75$). Columns two and three of Table (2) show a similar trend in behavior. Column three clearly demonstrates that using one outer drum wall temperature sensor is justifiable.

Table (2) Performance index (J_i) of the three estimators for the intervals (0-50), (50-487) and (0-537) min.

Measured Variables	J_i		
	50 min	487 min	537 min
T_1^*	1.7501	0.3495	0.4799
T_5^*	0.5938	0.161	0.2013
$T_1^* \& T_5^*$	0.2397	0.1752	0.1812

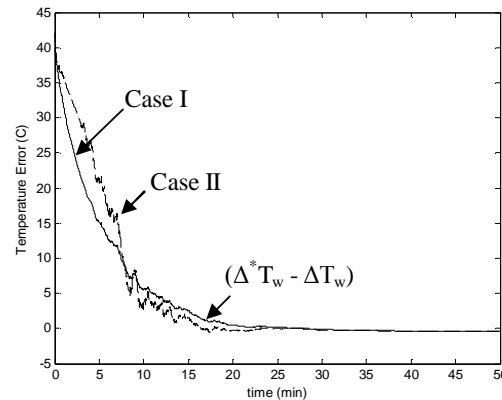


Figure (10) Temperature error response with two different initial conditions.

The tests shown in figures (10) and (7) are similar but with estimator initial conditions of $[100 \ 100 \ 100 \ 100 \ 100]^T$. The temperature error response (case I) indicates very good tracking and the estimator follows the input in less than 30 minutes. The figure also shows (case

II) that the estimator is capable of estimating the drum wall temperature and tracks the reference temperature even when random and unequal initial conditions of $[100\ 60\ 60\ 60\ 30]^T$ are used.

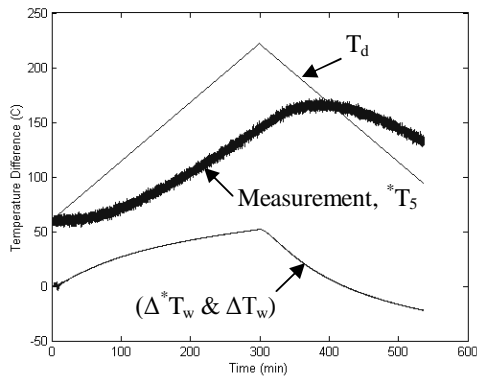


Figure (11) As in figure (7a) but with boiler shut-down after about 5 hours from heating start up.

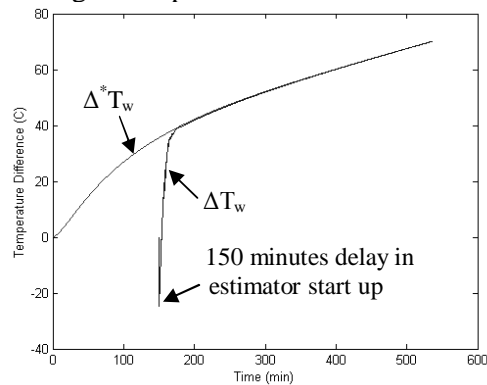


Figure (12) As in figure (7a) but the estimator is initiated 2.5 hours after boiler start up.

To demonstrate the performance of the estimator under other operating conditions, three cases were considered. The first case is that of a boiler shut-down after about 5 hours from heating start up. The estimator behavior is shown in figure (11). Such a case may arise if a decision is taken by the power station engineers to shut-down the boiler due to a failure alarm in any one of the plant's units. The estimator is based on the $*T_5$ measurement with estimator initial conditions of $[60\ 60\ 60\ 60\ 60]^T$. The second case study is

shown in figure (12) where for some reason or another estimator is started after 2.5 hours from boiler start up. The estimator uses $*T_5$ as temperature measurement and with initial conditions of $[60\ 60\ 60\ 60\ 60]^T$.

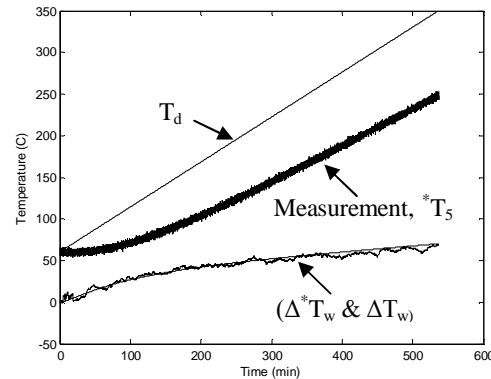


Figure (13) Estimator performance with 0.1 plant model noise uncertainty.

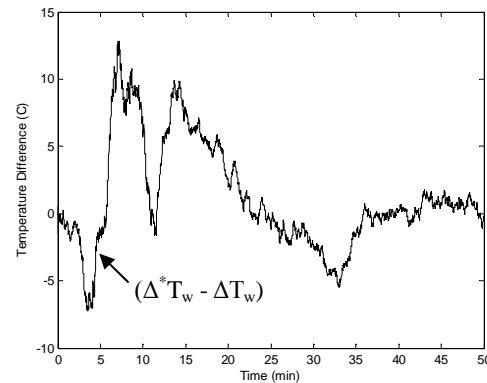


Figure (14) Typical temperature error response with 0.1 plant noise uncertainty.

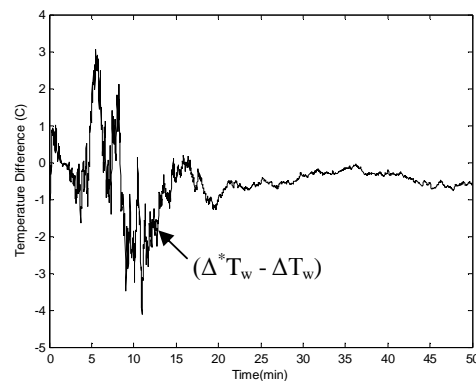


Figure (15) Typical temperature error response with 0.01 plant noise uncertainty.

Finally, the estimator performance is examined with the presence of process noise in the plant dynamic model. Using uncertainty (w_k) in the dynamic model (equation (8)), two sets of numerical tests were carried out as shown in figures (13) to (15) with uncertainty of 0.1 and 0.01. The temperature noise (v_k) was ± 2 °C in *T_5 for all tests. Figure (13) shows that the estimator estimates the drum wall temperature difference and tracks the reference temperature closely. Figure (14) shows that the maximum wall temperature difference between the estimated and the reference model temperatures is -7 and 13 °C. Since the plant noise is of a random nature, a series of tests were conducted and the maximum deviation in all these tests was within 30 °C temperature range for the first 15 minutes of the run time. In all these tests the estimator output is within 7% of the true value after 30 minutes from the start up. Reducing the plant noise uncertainty leads to reduces the estimation error. Figure (15) is a repeat the test shown in figure (14) but with plant model noise uncertainty of 0.01. The temperature difference error is within ± 4 °C.

7- Conclusions

A classical estimator (Kalman filter) was designed to estimate boiler drum temperature wall differential, a crucial issue in limiting drum's thermal stresses especially at the start up. The proposed system is simple in the sense that it requires a single thermocouple located at the outer surface of the drum and a software estimator. The model should be accurate enough to get good estimation in reasonably short time. The quality of the model affects the estimation. Many sets of initial conditions were used in the numerical experiments of the estimator. The estimator performance was as expected, rather slow at the beginning of

the estimation. It takes about 30 minutes to estimate wall temperature difference with an accuracy of ± 1 °C. The quality of the estimation increases from start up to finish. The results indicated robust estimator performance with regard to the variation in initial conditions. The performance of the estimator was not seriously influenced even with 100% error in initial conditions. Temperature estimation using software solution is simple and cheap as compared with hardware solution. Thus, attention must be paid to the application of the estimation techniques, which can provide solutions to many engineering problems especially those where the operating environment is harsh such as those of power station boiler drums. Future work is to be directed to improve the boiler drum model by including inner and outer surfaces heat transfer conditions.

References

- 1) Weisman, J. and Eckart, R., "Modern Power Plant Engineering", Prentice-Hall, Englewood Cliffs, (1984).
- 2) "AL-Mussaib Power Station Document", AL-Mussaib Thermal Power Plant Engineering Department, Ministry of Electricity, Baghdad, IRAQ.
- 3) Sorenson, H. W., "Kalman Filtering: Theory and Application", IEEE Press, New York, (1985).
- 4) Lumelsky, V. J., "Estimation and Prediction of Unmeasurable Variables in the Steel Mill Soaking Pit Control System", IEEE-Transactions on Automatic Control, Vol. AC-28, pp. 388-400, March, (1983).
- 5) Tylee, J. L., "On-Line Failure Detection in Nuclear Power Plant Instrumentation", IEEE Transactions on Automatic Control, Vol. AC-28, pp. 406-415, March, (1983).
- 6) Huisman, L., Beerkens, R. and Backx, T., "Estimation of Process Variables in a

- Glass Melting Furnace”, <http://www.tpd.tno.nl/Docs/DMP/glass-group/2001/posterleo2001.pdf>
- 7) Sa'id, W. K. and AL-Kubaissy, O. F., "Estimation of Unmeasurable Molten Metal Temperature of Induction Furnaces by Kalman Filtering Technique", 3rd National Conference on Computers, Control and Systems Eng. (CCSE), UOT, (2002).
 - 8) Fluerasu, A. and Sutton, M., "Kalman-Predictive-Proportional-Integral-Derivative (KPPID) Temperature Control", AIP Conference Proceeding, Vol. 684, No. 1, pp. 933-938, September 29, (2003).
 - 9) Ben-Yaacov, G. Z. and Bohn, J. G., "Methodology for Real-time Calculation of Temperature Rise and Dynamic Rating for Distribution System Duct Banks", IEEE-Transactions on Power Apparatus and Systems, Vol. PAS-101, No.12, pp. 4604-4610, December, (1982).
 - 10) Holman, J. P., "Heat Transfer", McGraw-Hill, Inc., (1989).
 - 11) Al-Ubaidy, M. A., "Charge Temperature Estimation of an Induction Furnace", M.Sc., Thesis, Al-Nahrain University, (1994).
 - 12) Oleiwi, B. K., "Kalman Estimator Design for the Boiler Drum Wall Temperature Differentials during Start Up", M.Sc., Thesis, University of Technology, (2005).
 - 13) Welch, G. and Bishop, G., "An Introduction to the Kalman Filter", ACM, Inc., (2006).
 - 14) Kanjilal, P. P., "Adaptive Prediction and Predictive Control", IEE Control Engineering Series 52, (1995).
 - 15) Girgis, A. A. and Brown, R. G., "Application of Kalman Filter in Computer Relaying", IEEE-Transactions on Power Apparatus and Systems, Vol. PAS-100, No. 7, pp. 3387-3397, July, (1981).